Melting of ultrathin copper nanobridges

J. W. Kang and H. J. Hwang

Chung-Ang University, Seoul, Korea, kok@semilab3.ee.cau.ac.kr

ABSTRACT

This study showed the various physical phenomena of ultrathin nanobridges, such as the melting and breaking of nanobridges using classical molecular dynamics simulations and a many-body potential function of the second-moment approximation of tight-binding scheme. Even if this study was confined within eight systems of ultrathin nanobridges, this study has disclosed some interesting features of nanobridges, and the caloric curves and diffusivities of nanobridges provided the information on the melting and breaking points of nanobridges.

Keywords: Ultrathin copper nanotube, Helical multi-shell structure, Atomistic simulation

1 INTRODUCTION

In nanoelectronic engineering, the mechanical, optical, and electrical properties of one-dimensional nanometer-scale wires have been investigated in the past decade [1-19]. The mechanical and electrical properties of metallic nanocontacts in which a neck of atoms just a few atomic diameters bridges two electrical contacts have been a subject of intensive research [4-15]. The results prepared by contacting a metal surface with the scanning tunneling microscope (STM) [6-10] and by other methods [11-15] have typically displayed a conductance quantized in steps of $2e^2 / h$, where e is the electron charge and h is Planck's constant. The mechanical properties of nanocontacts have shown that before the first yielding, nanowires preserve the elastic stage, and after that, the elongation deformation proceeds in alternating quasi-elastic and yielding stages [10,16]. The thermal properties of nanocontacts (or nanobridges) have to be investigated for device applications of nanocontacts. Therefore, the melting of infinite Pb [17] and Au [18] nanowires with periodic boundary conditions (PBC) along the axes of nanowires have been investigated via molecular dynamics (MD) simulations. However, previous works [17,18] have not been enough to provide the thermal properties of nanobridges, such as the melting and breaking of nanobridges. Therefore, this paper investigated the thermal properties of ultra-thin nanobridges, such as the melting and breaking of nanobridges, using a classical MD simulation.

2 COMPUTATIONAL METHODS

The interaction between copper atoms is described by a many-body potential function of the second-moment approximation of the tight-binding (SMA-TB) scheme [22] that has already been tested in nanoclusters and nanowires [16,19,20,23-26], etc. The potential reproduces many basic properties of crystalline and noncrystalline bulk phases and surfaces [23], gives a good insight into the structures and thermodynamics of metal clusters [25,26] and nanowires [16,24], and gives physical values in good agreement with experimental and theoretical values such as surface energies and diffusion energy barriers [16]. The cut off distance, 5.30 Å, is the average of the distance between the fourth and fifth nearest neighbors of perfect crystal.

In these MD simulations, we used the same MD methods which employed previously in studies on the cluster deposition and the structural motifs of Cu nanowire [16,19,20]. The MD timestep was 0.5 fs. The MD code uses the velocity Verlet algorithm, Gunsteren-Berendsen thermostat to keep constant temperature, a PBC along the wire axis, and neighbor lists to improve computing performance [21].

The nanostructures we studied have two supporting layers that are connected with both ends of the nanobridges. In this paper, structures connected with the supporting layers are called nanobridges and semi-infinite nanowire with the PBC is called nanowire. D and L in Table 1 denote the diameter and the length of nanobridges, respectively. The last layers at both supporting ends are rigid, and these fixed layers at both ends are assumed to be connected to the external agent. All the atoms in these layers are kept fixed during the MD simulations. Atoms in the following two layers adjacent to the fixed ones and those of the nanobridge were identified as dynamic atoms and were fully relaxed during the MD simulations. We considered eight different structures, which are described in Table 1. Since the ultrathin metal nanowires have been observed in face centered cubic (fcc) [28] and cylindrical multi-shell (CMS)-type structures [19,24], we have selected nanobridges with fcc or CMS-type structures, and the supporting layers have the same structures as those of the nanobridges. To describe CMS-type nanowires, we use the notation n - n'- n''- n''' introduced by Kondo and Takayanagi [9], when the nanowire consists of coaxial tubes with n, n', n'', n''' helical atom rows ($n > n' > n'' > n'''$). Since each shell of the CMS-type nanobridges is composed of the circular folding of {111} plane [19], their structures are similar to the {111} structure. Therefore, the CMS-type nanobridges are connected with the supporting layers with {111} planes. Nanobridges with different diameter were simulated under the conditions of the same structure and the same length..

3 RESULTS AND DISCUSSION

The relaxed structures of nanobridges were obtained from the MD simulations using all initial nanobridges in Table 1, which have been performed during 1 ns at 300 K. The CMS-type nanobridges have maintained their structures between the supporting layers with {111} planes. However, one or two layers of the CMS-type nanobridge contacting the supporting layers were transformed into {111} structure and the other regions have preserved the CMS-type structure. These results are in good agreement with those obtained from experiments [9].

Each system relaxed by MD simulations of 1 ns at 300 K was heated by uniformly scaling the atomic velocities. The mean kinetic temperature $k_B T = [2/(3N-6)]\left\langle \sum_{i=1}^{N} (mv_i^2/2) \right\rangle$, where the angular brackets denote averaging over time and k_B is the Boltzman constant, supply the energy to atoms in nanobridges. The MD runs of 20,000 timesteps were performed with each temperature step from 300 K, and so, the average temperature ascent rate is 0.1 K/ps.

Figure 1 shows the caloric curves and diffusivities of the CMS 16-11-6-1 nanowire as a function of temperature. The caloric curve of the CMS 16-11-6-1 nanowire close to one-dimensional system is in the regime of the pseudo-first-order transitions and the jump in the caloric curve is apparent. The slope of the caloric curve of the CMS 16-11-6-1 corresponds to the Dulong-Petit specific heat, and the M and B points indicate pronouncedly upward and downward points in the caloric curve, which are related the melting and breaking of nanowire. The temperatures corresponding to pronouncedly upward curves related to the latent heat are defined as the melting points. In the caloric curve of the CMS 16-11-6-1 nanowire, it is divided into four regions. The first region ranges below the M point, where the ultrathin nanowire is solid. The second region is the M point that caloric curve exhibits an upward curvature, where the specific heat pronouncedly increases by the beginning of melting. This upward curvature is associated with the loss of the solid rigidity of nanowire, the latent heat. The third region is between the M and B points, where the ultrathin nanowire is in the melting, and the slope is the same with that in the first region. The last region is the B point that the ultra-thin nanowire is broken and then spherical cluster is formed in the conditions of MD simulation. The slope in the caloric curve of the CMS 16-11-6-1 nanowire is always the same with those in the first and third regions. The specific heat for the SMA-TB potential used is 0.389 J/g °C obtained from the caloric curves and is in good agreement with the experimental value, 0.385 J/g °C [29]. The melting temperature of the CMS 16-11-6-1 nanowires is much lower than that of the bulk. Thus properties of the caloric curve of nanowires except for the downward curvatures are in an excellent agreement with the previous works for nanowires [17,18] and nanoclusters [27]. The previous works [17,18] have not shown the breaking of nanowires, but have shown only the melting of nanowires.

Figure 2 shows snapshots of the CMS 16-11-6-1 nanowire for various temperatures, and these are very helpful for understand the melting and breaking behaviors of the CMS 16-11-6-1 nanowires. Figure 2(a) shows that the structure of its solid region at 450 K maintains its initial structure. However, at 580 K, the melting temperature of the nanowire, the structure is deformed as shown in Fig. 2(b). Figure 2(c) shows that at 700 K, the nanowire is in the melting state and that the structure is similar to an amorphous state. Figure 2(d) shows the structure just before the breaking of the nanowire at 800 K. As the temperature approaches near the breaking point of the nanowire, the neck of the nanowire becomes more and more narrow and finally is broken as the fuse burns out at high temperature. As mentioned above, Fig. 2(e) shows a spherical cluster formed after the breaking of the nanowire. The spherical cluster is formed because of the PBC applied to the supercell.

In our simulations, the properties of nanobridges were similar to those of nanowire. The caloric curves of nanobridges were generally similar to that of nanowires or nanoclusters [16,27], and the M and B points in the caloric curves of nanobridges also were found as the upward and downward curvatures. When the temperature of nanobridge reached its M point, the nanobridge came in melting and then the tension in the nanobridge gradually decreased.

As the temperature increases, the diameter of the neck of nanobridge decreases because atoms in the nanobridge migrate to the supporting layers. The structures at the M point are in the melting. When the temperature reaches the B point, the nanobridge was broken and at the same time, atoms were swiftly accumulated on the supporting layers due to the tension just before breaking.

Therefore, the B point of nanobridge can be also defined by the variation of atomistic mobility as a function of temperature, as shown in Fig. 1. The corresponding diffusion coefficient was evaluated for each temperature as the $(1/6t)\left\langle \left\langle \sum_{i=1}^{N} |r_i(t) - r_i(0)|^2 \right\rangle \right\rangle$, where $r_i(0)$ and $r_i(t)$ are the vector positions of ith atom at time = 0 and t, respectively. Figure 3 shows the diffusivities of nanobridges and CMS 16-11-6-1 nanowire compared with that of the bulk for the melting temperature more or less. At low temperatures (< 500 K), the diffusivities of atoms in nanobridges and nanowire are higher than that of atoms in the bulk [28]. The variations of diffusivity before the breaking of nanobridges are in a good agreement with that of clusters [27] or nanowires [18]. The diffusivities of the CMS 16-11-6-1 nanowire slowly increase until the M point, and show pronouncedly upward curvature at the M point. This reason is that due to the melting at the M point, atoms in the CMS 16-11-6-1 nanowire rapidly migrated to both directions along the wire axis. Above the melting point, atoms on the surface of nanobridges were gradually piled up on the supporting layers. Therefore, after M points, atoms in nanobridges began to migrate to the supporting layers, and this migration became major factor in diffusivity ascension. While the atoms of the CMS 16-11-6-1 nanowire applied to the PBC freely moved along the wire axis, the atoms of nanobridges lay thick on the supporting layers. Therefore,

the diffusivities of nanobridges are less than that of the CMS 16-11-6-1 nanowire. However, in Fig. 3, the diffusivities of nanobridges after their M points are in a good agreement with the experimental values of diffusivity of liquid Cu [28].

When the temperature reached the B point of nanobridge, the nanobridge was broken and at the same time, atoms swiftly were piled up on the supporting layers due to the tension just before the breaking. Therefore, the diffusivities of nanobridges just after the B points decrease. However, as the temperatures increase higher than the B points of nanobridges, the diffusivities of nanobridges again increase. In the case of the CMS 16-11-6-1 nanowires, spherical nanocluster was formed just after the B point, and then the diffusivities of the system also decrease as shown in Figs. 1 and 3. As the temperatures of the CMS 16-11-6-1 nanowire increase over the B point, diffusivities again increase.

In the cases of A1, B1, C1, and D1, the M points were not observed in our simulations but the B points were observed. We can see that the M point of nanobridge is closely related to the linear density and diameter of nanobridge in Fig. 4. In cluster science, the melting temperature depends on the cluster size and is expressed by following form [18]:

$$T_{mc} = T_b - c / D_c , \qquad (3\text{-}1)$$

where T_{mc} is the melting temperature for the spherical nanoparticle of diameter D_c, T_b is the bulk melting temperature, and c is a constant. From our results, the melting temperature of nanobridges is expressed by approximately as follows:

$$T_{mn} = T_b - n / D_n , \qquad (3\text{-}2)$$

where T_{mn} is the melting temperature for the nanobridge with diameter, D_n, and n is a constant. The upper graph of Fig. 4(a) shows the T_{mn} with the line fitted by Eq. (3-2) originating at the T_b obtained from the SMA-TB potential, 1490 K [22].

Since the breaking temperature of nanobridge can be dependent on the diameter of nanobridge, linear density of nanobridge, crystallographic orientation, shapes in the different direction, etc., our simulation results in this paper are not enough to provide some physical properties of the breaking of nanobridges due to thermal energies. However, in our simulation results, if we assume that the B points of nanobridges depend on the diameters of nanobridges, the form of Eq. (3-2) could express those. Therefore, the bottom graph of Fig. 4(a) shows the B points with the solid line fitted by Eq. (3-2) originating at the T_b obtained from the SMA-TB potential. For the ultrathin nanobridges, since it has been well known that the CMS-type structures are more stable than the other structures, the M and B points of the CMS-type nanobridges are higher than those of the other nanobridges. However, for the larger nanowires, since the nanobridges with *fcc* structure are more stable than the CMS-type nanobridges, the dashed line of Fig. 4(a), the line fitted for the CMS-type nanobridges, originates at near 900 K. Figure 4(b) shows the M and B points as a function of the linear densities of nanobridges, and the M and B points of nanobridges are linearly proportional with the linear density of nanobridge.

4 CONCLUSION

The previous studies on nanoclusters [27] and infinite nanowires [17,18] have shown the physical phenomena related to only the melting of nanoclusters and nanowires. This study showed the various physical phenomena of ultrathin nanobridges, such as the melting and breaking of nanobridges using classical molecular dynamics simulations. Even if this study was confined within eight systems of ultrathin nanobridges, this study has disclosed some interesting features of nanobridges, and the caloric curves and diffusivities of nanobridges provided the information on the melting and breaking points of nanobridges. However, more detail works are still necessary to investigate on the properties of the breaking of nanobridges.

Table 1. . Structures of ultrathin Cu nanobridges.

	Supporting layer	Nanobridge	D (Å)	L (Å)	The linear density (10^{-16} kg/m)
A1	{100}	{100}	10.2	61.449	73.0
A2	{100}	{100}	15.0	61.449	166.5
B1	{110}	{110}	10.2	42.452	80.3
B2	{110}	{110}	15.0	42.452	188.8
C1	{111}	{111}	10.2	70.956	73.2
C2	{111}	{111}	15.0	70.956	163.9
D1	{111}	CMS 6-1	4.9	64.294	34.3
D2	{111}	CMS 11-6-1	10.2	64.294	87.7

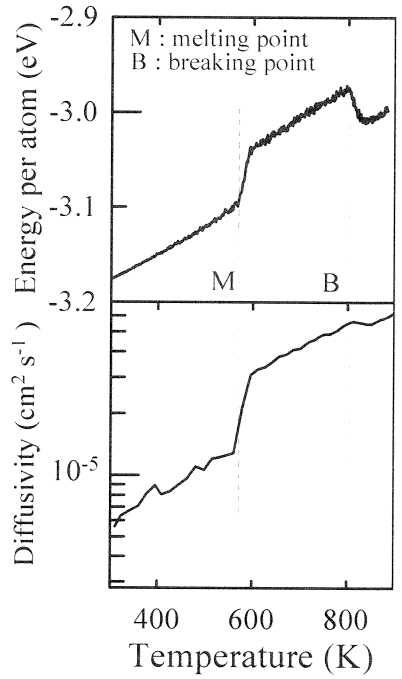

Figure 1. Caloric curve and diffusivities of the CMS 16-11-6-1 nanowire as a functions of temperature

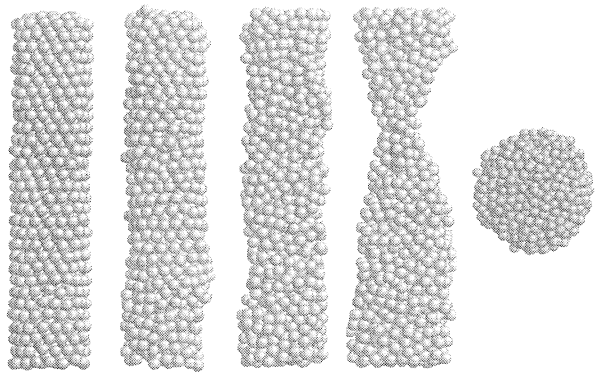

(a) (b) (c) (d) (e)

Figure 2. Snapshots of the CMS 16-11-6-1 nanowire for temperatures of (a) 450 K, (b) 580 K, (c) 700 K, (d) 800 K, and (e) 850 K.

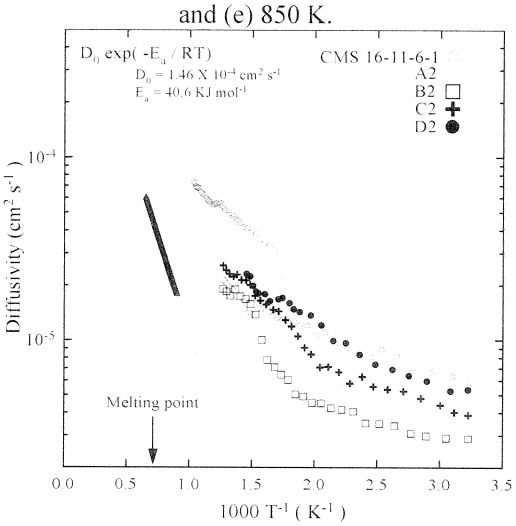

Figure 3. Diffusivity of nanobridges, A2, B2, C2, and D2, and the CMS 16-11-6-1 nanowries. The diffusivities of nanobridges and nanowire are compared with that of the bulk for melting temperature more or less.

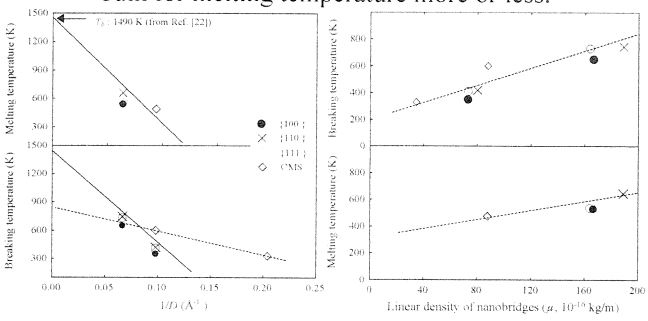

Figure 4. (a) The M and B points of nanobridges with curves fitted by Eq. (3-2). (b) The M and B points of nanobridges as a function of the linear density of nanobridges.

REFERENCES

[1]R.A. Webb, S. Washburn, C.P. Umbach, and R.B. Laibowitz, Phys. Rev. Lett. 54, 2696, 1985.

[2]S. Iijima, Nature 354, 56, 1991.

[3]M. Bockrath, D.H. Cobden, P.L. McEuen, N.G. Chopra, A. Zettl, A. Thess, and R.E. Smalley. Science 275, 1922, 1997.

[4]N. Agrait, G. Rubio, and S. Vieira, Phys. Rev. Lett. 74, 3995 1995.

[5]J.M. Krans, J.M. van Ruitenbeek, V.V. Fisun, I.K. Yanson, and L.J. de Jongh, Nature 357, 767, 1995.

[6]L. Olesen, E. Lagsgaard, I. Stensgaard, F. Besenbacher, J. Schiotz, P. Stoltze, K. W. Jacobsen, and J.K. Norskov, Phys. Rev. Lett. 72, 2251 1994.

[7]J.I. Pascual, J. Mendex, J. Gomez-Herrero, A.M. Baro, N. Garcia, U. Landman, W.D. Luedtke, E.N. Bogachek, and H.P. Cheng, Science 267, 1793 1995.

[8]M. Diaz, J.L. Costa-Kramer, A.L. Escobar, N. Leon, and A. Correia, Nanotechnology 13, 43, 2002.

[9]Y. Kondo and K. Takayanagi, Phys. Rev. Lett. 79, 3455, 1997; H. Ohnishi and Y. Kondo, K. Takayanagi, Nature 395, 780, 1998; Y. Kondo and K. Takayanagi, Science 289, 606, 2000.

[10]G. Rubio, N. Agrait, and S. Vieira, Phys. Rev. Lett. 76, 2302, 1996.

[11]C.J. Muller, J.M. Krans, T.N. Todorov, and M.A. Reed, Phys. Rev. B 53, 1022, 1996.

[12]U. Landman, W.D. Luedtke, B.E. Salisbury, and R.L. Whetten, Phys. Rev. Lett. 77, 1362, 1996.

[13]J.L. Costa-Kramern, N. Garicia, R. Garcia-Mochales, and P.A. Serena, Surf. Sci. 342, L1144, 1995.

[14]K. Hansen, E. Lagsgaard, I. Stensgaard, and F. Besebacher, Phys. Rev. B 56, 2208, 1997.

[15]H. Yasuda and A. Sakai, Phys. Rev. B 56, 1069, 1997.

[16]J.W. Kang and H.J. Hwang, Nanotechnology 12, 295, 2001.

[17]O. Gulseren, F. Ercolessi, and E. Tosatti, Phys. Rev. B 51, 7377, 1995.

[18]G. Bilalbegovic, Solid State Commu. 115, 73, 2000.

[19]J.W. Kang and H.J. Hwang, Mol. Sim. (in press).

[20]J.W. Kang and H.J. Hwang,Comp. Mater. Sci. 21, 509, 2001; J.W. Kang, K.S. Choi, K.R. Byun, and H.J. Hwang, J. Vac. Sci. Technol. A 19, 1902, 2001.

[21]M. P. Allen and D. J. Tildesley, "Computer Simulation of Liquids," (Clarendon press, Oxford, 1987).

[22]F. Cleri and V. Rosato, Phys. Rev. B 48, 22, 1993.

[23]M. Guillope and B. Legrand, Surf. Sci. 215, 577, 1989.

[24]B Wang, S. Yin, G. Wang, and J. Zhao, J. Phys.: Condens. Matter 13, L403, 2001.

[25]Y.J. Lee, J.Y. Maeng, E.K. Lee, B. Kim, S. Kim, and K.K. Han, J. Comput. Chem. 21, 380, 2000.

[26]Y.J. Lee, E.K. Lee, S. Kim, and R.M. Nieminen, Phys. Rev. Lett. 86, 999, 2001.

[27]J. Mei and J. W. Davenport, Phys. Rev. B 42, 9682, 1990.

[28]R. Hultgren, P. D. Desai, D. T. Hawkins, M. Gleiser and Kelly K K, "Selected Values of the Thermodynamics Properties of Binary Alloys" (American Society for Metals, Metal Park, 1973).